Electronic Supplementary Information

Zeolites with isolated-framework and oligomeric-extraframework hafnium species characterized with pair distribution function analysis

Takayuki Iida[1,2], *Koji Ohara*[3], *Yuriy Román-Leshkov*[2*], and *Toru Wakihara*[1*]

1) Department of Chemical System Engineering, The University of Tokyo, 7-3-1 Hongo, Bunkyo-ku, Tokyo 113-8656, Japan

2) Department of Chemical Engineering, Massachusetts Institute of Technology, 25 Ames Street, Cambridge, Massachusetts 02139, United States of America

3) Japan Synchrotron Radiation Research Institute/SPring-8, Kouto 1-1-1, Sayo-gun, Hyogo 679-5198, Japan

*Corresponding Author: yroman@mit.edu, wakihara@chemsys.t.u-tokyo.ac.jp;

Phone: Prof. Yuriy Román-Leshkov (+1) 617-253-7090, Prof. Toru Wakihara (+81) 3-5841-7368

Table of contents

1. Experimentals

1.1 Reagents

Hafnium cyclopentadiene chloride ($Hf(Cp)_2Cl_2$; Sigma-Aldrich), nitric acid (60 wt%; Sigma-Aldrich), aluminosilicate *BEA zeolite (Si/Al = 12.5, CP814E*, Zeolyst), HfO_2 (Sigma-Aldrich), benzaldehyde (Wako Chemicals), acetone (Wako Chemicals), toluene (Wako Chemicals), tri-tert-butylbenzene (Wako Chemicals), tetraethoxyorthosilicate (TEOS; Alfa-Aesar), tetraethylammonium hydroxide (35 wt%; Sigma-Aldrich), hydrofluoric acid (48 wt%, Sigma-Aldrich), tin dimethyl dichloride (Me_2SnCl_2; Sigma-Aldrich) were used as purchased. Air (dry grade) was purchased from Airgas.

1.2 Synthesis of the catalysts

Hf-beta(post) was synthesized as follows. First, removal of framework aluminum from the aluminosilicate *BEA zeolite was performed by immersing the *BEA zeolites into nitric acid, and heating the suspension inside a Teflon®-lined steel autoclave for overnight. After collecting the solid by filtration and washing with deionized water (the product denoted as DeAl-beta), the zeolite was degassed under vacuum at 400°C for overnight. The dried zeolite was transferred and stored inside a glovebox. Into a Teflon®-lined autoclave, the degassed DeAl-beta, metal precursor ($Hf(Cp)_2Cl_2$ or Me_2SnCl_2), and

toluene were added, and the container was sealed inside the glovebox. The mixtures were heated at 160°C for 16 h to graft the metal precursor to the framework sites. The solid was collected by filtration, washed with hexane, and calcined in the oven at 550°C for 3 h under dry air flow (100 mL/min) after 3 h of ramping period. A second acid treatment was performed to the product after the calcination treatment following the same procedure described for removing the framework Al.

Si-beta(F), pure silica *BEA zeolite, was prepared following the procedures reported in previous works[1], with ingredient molar composition of SiO_2 : TEAOH : HF: H_2O = 1 : 0.5 : 0.5 : 7.5. For preparing HfO_x/Si-beta, incipient-wetness impregnation was performed with an ethanol solution containing the desired amount of $HfCp_2Cl_2$. The dried sample was calcined at 550˚C for 3 h under dry air flow (100 mL/min).

1.3 Catalyst characterization

Powder X-ray diffraction (XRD) patterns were collected using Bruker D8 diffractometer with Nickel-filtered Cu Ka radiation (λ = 1.5418 Å) for a 2θ range of 3°–50°. N_2 physisorption was carried out on Quantachrome Autosorb iQ-2 automated gas sorption system. All samples were degassed under vacuum prior to use (350°C) and the measurement was conducted at liquid nitrogen temperature (-196°C).

The activity for aldol condensation between benzaldehyde and acetone was measured

using the conditions based on a previous report[2]. GC-FID (Shimadzu 2014) fitted with DB-1701 column (Agilent) was used for quantification of the reactant/products. Tri-tert-butylbenzene was used as an internal standard.

The high-energy X-ray Total Scattering (HEXTS) measurements were performed on powder sample in a quartz capillary at room temperature using a horizontal two-axis diffractometer at the BL04B2 high-energy X-ray diffraction beamline (SPring-8, Japan). The energy of incident X-rays was 61.43 keV (λ = 0.2018 Å). The maximum Q ($Q = 4\pi \sin\theta / \lambda$), Q_{max}, collected in this study was 20 $Å^{-1}$. The obtained data were subjected to well-established analysis procedures, such as absorption, background, polarization and Compton scattering corrections, and subsequently normalized to give a Faber–Ziman total structure factor $S(Q)$[3,4]. These collected data were used to calculate the (reduced) pair distribution function, $G(r)$, using the following function:

$$G(r) = 4\pi r[\rho(r) - \rho_0] = \frac{2}{\pi}\int_{Qmin}^{Qmax} Q[S(Q) - 1]\sin(Qr)dQ,$$

where ρ is the atomic number density.

The theoretical PDFs were calculated using PDFgui software[5], and information regarding various crystal structures were taken from the following literatures; cubic[6], monoclinic[7], orthorhombic[8] HfO_2 and cassiterite[9].

The following definitions were used to quantify the catalytic testing results:

Conversion [%] = moles of reactant consumed / moles of reactant fed × 100

Selectivity [%] = moles of product / moles of reactant consumed × 100

2. Theory and the calculation methods for d-PDF analysis

An unique feature of PDF is its linearity[10], as shown in eq (1), to describe the pair distribution function, $G(r)$, of a binary phase admixture of pure phase A and pure phase B by a linear addition of each of the pair distribution functions, $G(r)$.

$$G_{Mixture}(r) = x_A G_A(r) + x_B G_B(r) + x_{A-B} G_{A-B}(r) \cdots (1)$$

Where x_A, x_B, and x_{A-B} are coefficients and $G_{Mixture}(r), G_A(r), G_B(r), and\ G_{A-B}(r)$ represent the pair distribution functions describing the structure of the mixture, phase A, phase B, and the interatomic correlations between phases A and B. When the phases are totally independent (for example, having no atomic connectivity by chemical bondings), the following approximation holds[11];

$$G_{A-B}(r) = 0 \cdots (2)$$

By modifying this equation as shown in Eq (3) below, and calculating the difference in the PDFs of mixture and B (as shown in the right side eq (3)), the structure of phase A can be extracted:

$$x_A G_A(r) \cong G_{Mixture}(r) - x_B G_B(r) \cdots (3)$$

There are two things to be taken into account for the calculation of d-PDFs regarding heteroatom-containing zeolites.

1) For heteroatom-containing zeolites, the assumption made in eq (2) does not hold

because there is a direct connectivity between the heteroatom and the zeolite, and thereby, the PDF describing the surrounding environment of the heteroatom (for example Hf) including the interatomic correlations with the zeolite framework, $G_{Hf-}(r)$, is extracted from the right side of eq (3). That is, eq (3) can be fixed to the following form.

$$x_A G_{Hf-}(r) = G_{Mixture}(r) - x_B G_{Zeolite}(r) \cdots (4)$$

2) In X-ray experiments, the scattering factors are functions of wavenumber vector Q, and thereby, assumption that x_B stays constant does not hold in the strict sense. Thereby, in this work, $x_B G_{Zeolite}(r)$ was calculated by the following Fourier transformation equation;

$$x_B G_{Zeolite}(r) = \frac{2}{\pi}\int_{Qmin}^{Qmax} Q\left[\frac{{c_B}^2 < f_B(Q) >^2}{< f_{Mixture}(Q) >^2} F_{Zeolite}(Q)\right]\sin(Qr)dQ \cdots (5)$$

Where,

$$F_{Zeolite}(Q) = S_{Zeolite}(Q) - 1 \cdots (6)$$

c_B represents the total the atomic composition of elements in phase B (in this case zeolites) out of the whole mixture (that is the mixture of zeolite and hafnium oxide phases), and $< f_B(Q) >$, $< f_{Mixture}(Q) >$ can be calculated based on the following equations.

$$< f_B(Q)^2 > = (\sum_i^B c_i f_i)^2 \cdots (7)$$

$$< f_{Mixture}(Q) >^2 = (\sum_i^{Mixture} c_i f_i)^2 \cdots (8)$$

Where c_i represents the atomic composition of element i, and f_i represents the X-ray scattering factor of element i.

Table S1. Results for elemental analyses of various catalysts

Catalyst	Si/Hf	Si/Sn	Si/Al
Hf-beta(post)	37	-	>1000
Hf-beta(post)_AT	180	-	>1000
HfO_x/Si-beta(F)	230	-	>1000
Sn-beta(post)	-	59	>1000
Sn-beta(post)_AT	-	93	>1000

Table S2. Textural properties of various catalysts

Catalyst	BET specific surface area [m^2 g^{-1}]	Micropore volume [cc g^{-1}]
Al-beta	644	0.17
DeAl-beta	513	0.14
Hf-beta(post)	547	0.16
Hf-beta(post)_AT	577	0.17
Si-beta(F)	554	0.21
HfO_x/Si-beta(F)	531	0.20

*Calculated using *t*-plot method

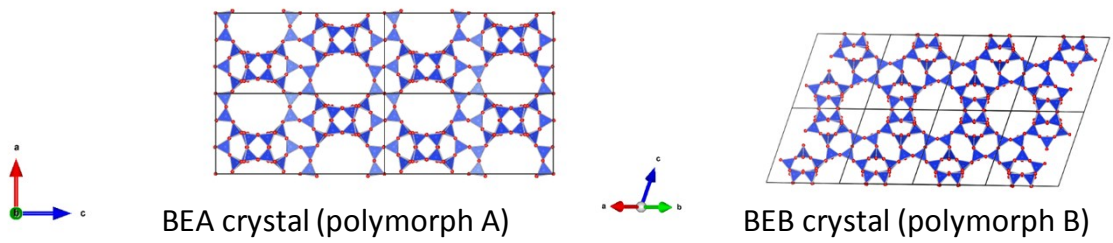

Figure S1. Crystal models of BEA and BEB zeolite polymorphs.

*BEA zeolites are obtained as an intermixture of both BEA and BEB crystal structure polymorphs. Information of the crystal structures were obtained from International Zeolite Association Structure Commission Database.

(http://www.iza-structure.org/databases/)

BEA crystal; (a = 12.66139 Å, b = 12.66139 Å, c = 26.40612Å, α=β=γ＝90°)

BEB crystal; (a = 17.89654 Å, b = 17.92002 Å, c = 14.32815 Å, α＝90°,β＝114.803°,γ＝90°)

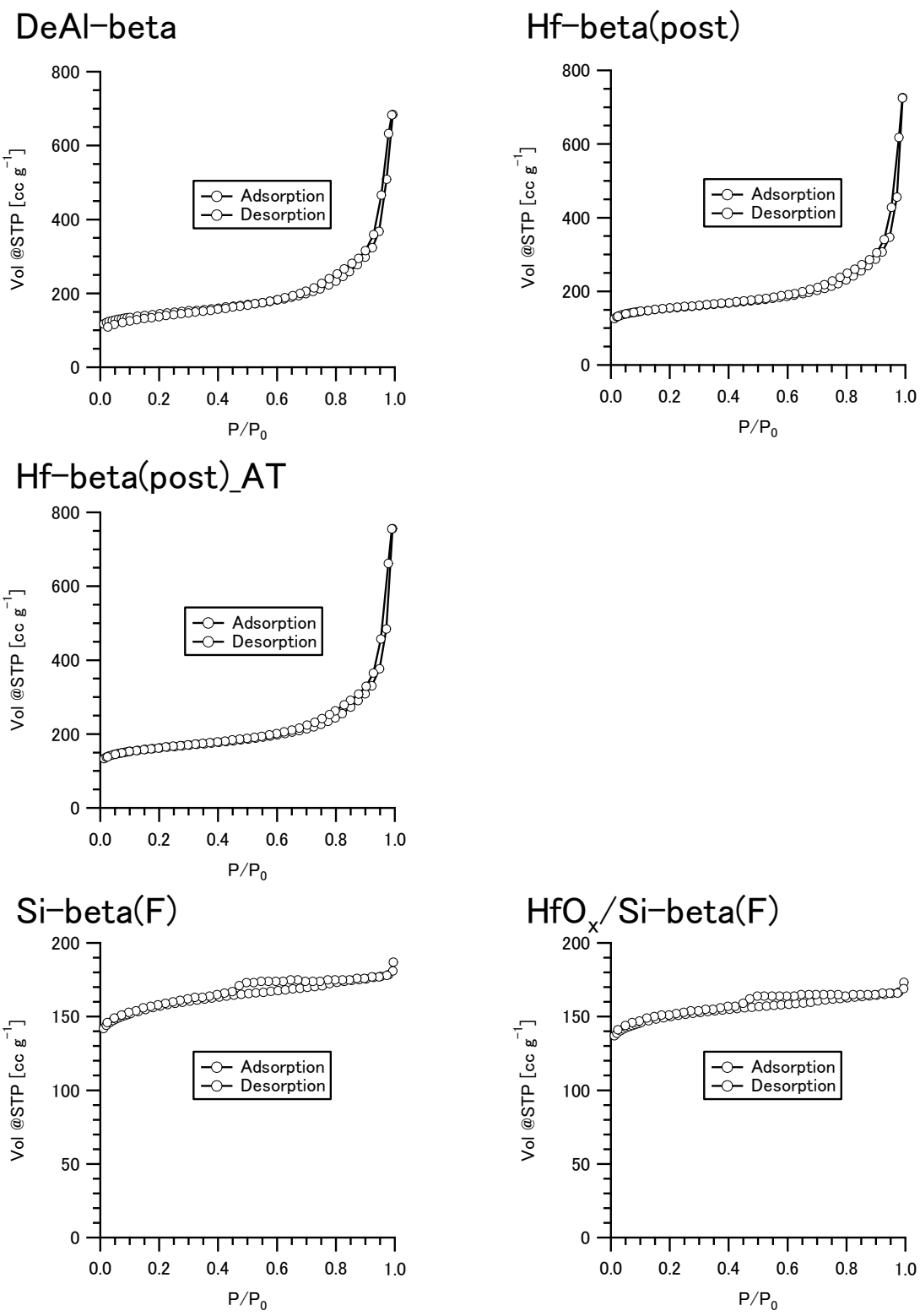

Figure S2. N_2 adsorption desorption isotherms of zeolite samples.

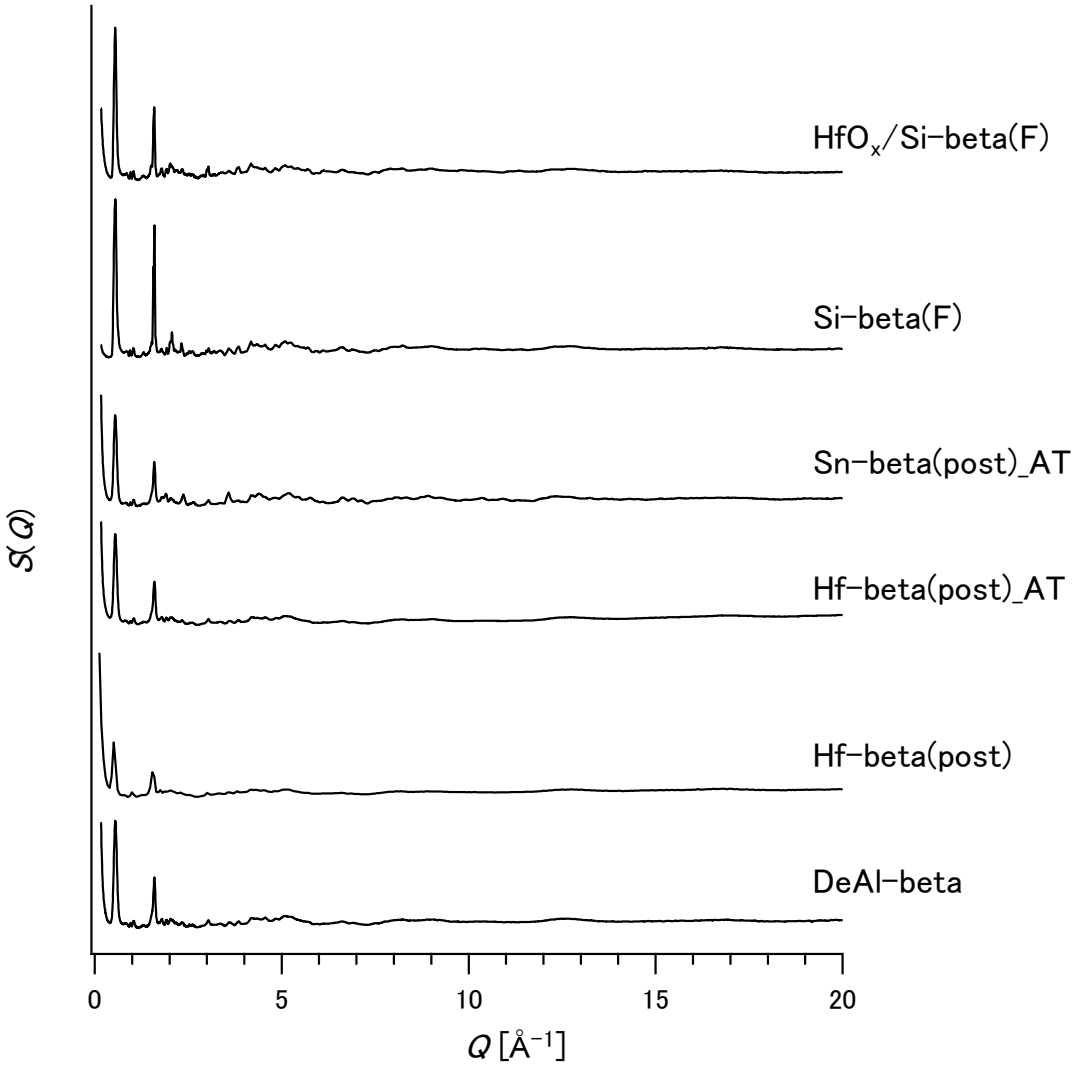

Figure S3. Faber-Ziman total structure factors, $S(Q)$, of the zeolites used in this paper.

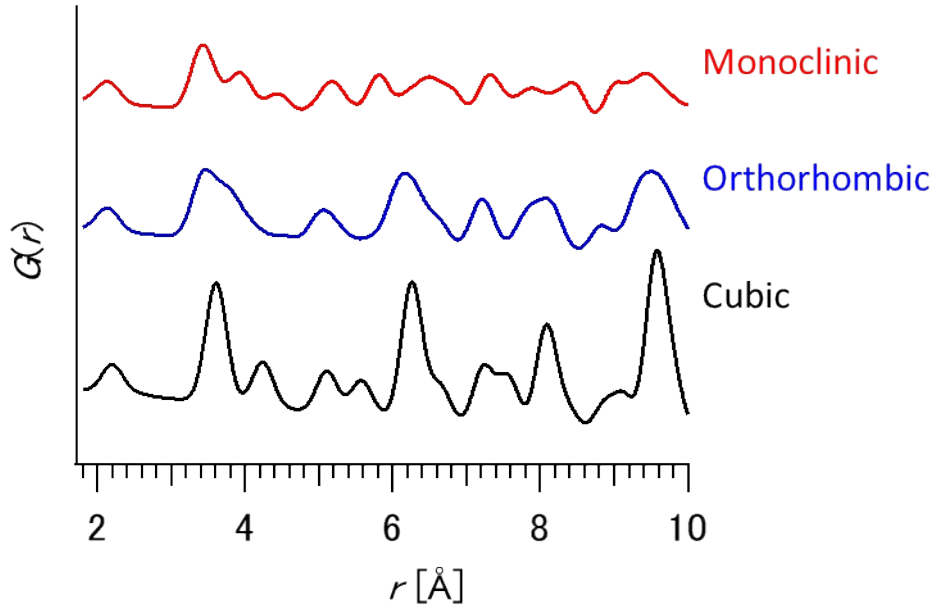

Figure S4. Comparison of the PDFs from different HfO_2 crystal structures.

The calculations were performed using PDFgui software[5].

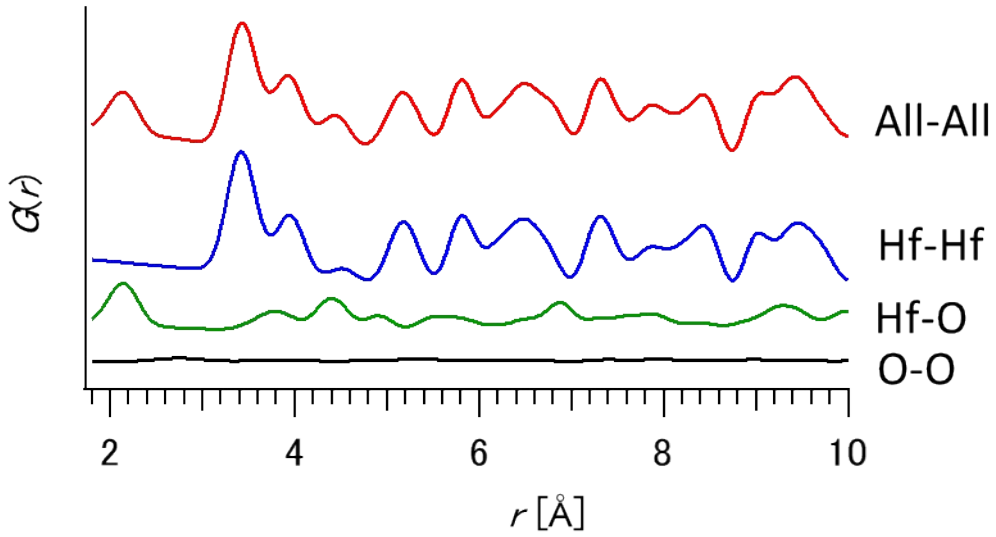

Figure S5. Assignment of the correlation peaks in the theoretical PDF of HfO_2 (monoclinic phase) made using the PDFgui software[5].

For example, Hf-Hf shows the probability of finding Hf-Hf distance at a given distance, *r*. Most correlations visible were found to originate from Hf-Hf or Hf-O correlations (at 2.0 and 4.4 Å) due to the relatively large X-ray scattering factor by Hf compared to O.

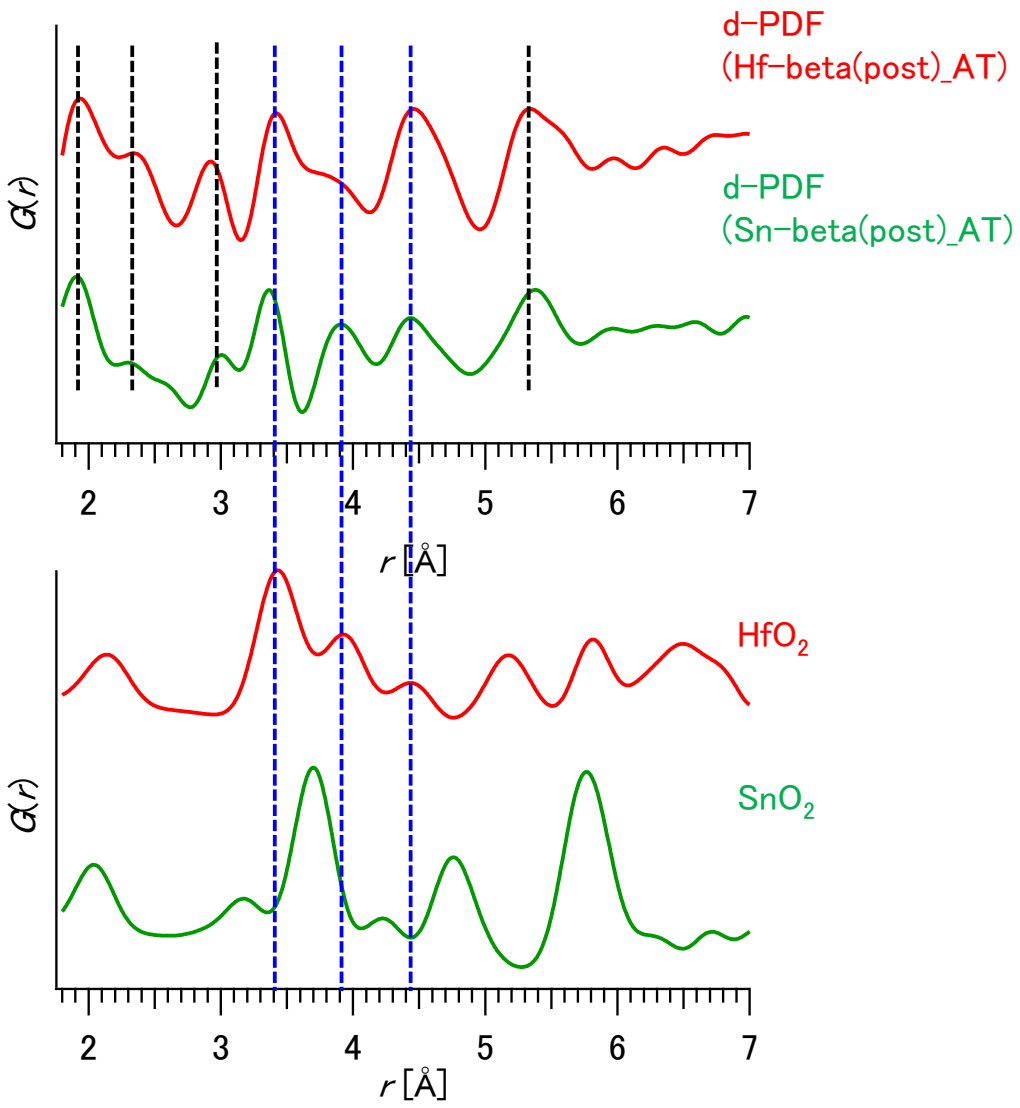

Figure S6. d-PDF comparison of Hf-beta(post)_AT and Sn-beta(post)_AT (top) in reference to the theoretical PDFs of *m*-HfO_2 and SnO_2 (cassiterite).

The blue dashed lines compare the peak positions in the d-PDF analysis, and with the correlations originating from *m*-HfO_2 in the distances between 3 ~ 4.5 Å. The black dashed lines compare the peak positions in the d-PDF analysis between Hf-beta(post)_AT and Sn-beta(post)_AT at the other distances.

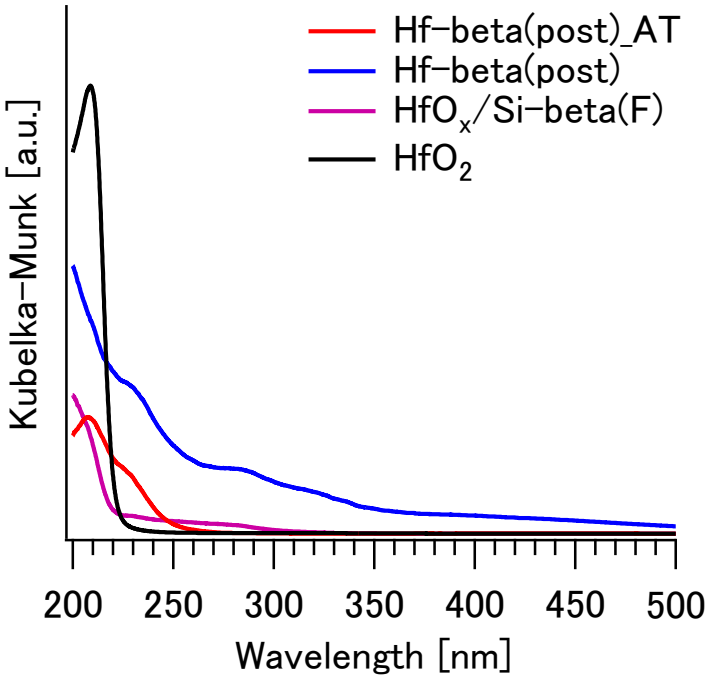

Figure S7. DR UV-vis spectra of various *BEA zeolites with hafnium in reference to that of bulk *m*-HfO_2.

References

1 M. A. Camblor, A. Corma and S. Valencia, Spontaneous nucleation and growth of pure silica zeolite-β free of connectivity defects, *Chem. Commun.*, 1996, 2365.

2 J. D. Lewis, S. Van De Vyver and Y. Román-Leshkov, Acid-Base Pairs in Lewis Acidic Zeolites Promote Direct Aldol Reactions by Soft Enolization, *Angew. Chem. Int. Ed.*, 2015, **54**, 9835–9838.

3 T. E. Faber and J. M. Ziman, A theory of the electrical properties of liquid metals, *Philos. Mag.*, 1965, **11**, 153–173.

4 S. Kohara, M. Itou, K. Suzuya, Y. Inamura, Y. Sakurai, Y. Ohishi and M. Takata, Structural studies of disordered materials using high-energy x-ray diffraction from ambient to extreme conditions, *J. Phys. Condens. Matter*, 2007, **19**, 506101.

5 C. L. Farrow, P. Juhas, J. W. Liu, D. Bryndin, E. S. Božin, J. Bloch, T. Proffen and S. J. L. Billinge, PDFfit2 and PDFgui: computer programs for studying nanostructure in crystals., *J. Phys. Condens. Matter*, 2007, **19**, 335219.

6 R. W. G. Wyckoff, *Crystal Structures Second Edition*, 1965.

7 R. Ruh and P. W. R. Corfield, Crystal structure of monoclinic hafnia and comparison with monoclinic zirconia Locality: synthetic, *J. Am. Ceram. Soc.*, 1970, **53**, 126–129.

8 O. Ohtaka, T. Yamanaka and S. Kume, Synthesis and X-ray structural analysis by the Rietveld method of orthorhombic hafnia, *Nippon Seramikkusu Kyokai Gakujutsu Ronbunshi*, 1991, **99**, 826–827.

9 W. H. Baur and A. A. Khan, Rutile-Type Compounds. VI. Si O2, Ge O2 and a Comparison with other Rutile-Type Structures, *Acta Crystallogr. B*, 1971, **27**, 2133–2139.

10 S. J. L. Billinge, Nanoscale structural order from the atomic pair distribution function (PDF): There's plenty of room in the middle, *J. Solid State Chem.*, 2008, **181**, 1695–1700.

11 T. Proffen, S. J. L. Billinge, T. Egami and D. Louca, Structural analysis of complex materials using the atomic pair distribution function – a practical guide, *Zeitschrift für Krist.*, 2003, **218**, 132–143.